Pol. J. Environ. Stud. Vol. XX, No. X (XXXX), 1-12
DOI: *10.15244/pjoes/221055* ONLINE PUBLICATION DATE: 2026-09-21

Original Research

Optimizing Tree Species Classification by Leveraging Median Filtering and Hybrid Feature Sets from Worldview Satellite Imagery

Huaipeng Liu[1]*, Jiaxin Lu[1], Xiaoqing Zuo[2], Chang Liu[1]

[1]School of Geography and Tourism, Luoyang Normal University, Luoyang, Henan Province, 471934, China
[2]School of Resources and Environmental Engineering, Hefei University of Technology, Hefei, Anhui Province, 230009, China

Received: 11 January 2026
Accepted: 23 April 2026

Abstract

The high-precision tree species identification results based on remote sensing are of importance in forest inventory, management, and biodiversity protection. To evaluate whether the median filtering technique can effectively improve tree species identification accuracy, this study utilized WorldView-2 and WorldView-3 imagery as data sources and applied different sizes of filter kernels to them. Subsequently, tree species classification was performed using the random forest (RF) and Extreme Gradient Boosting (XGBoost) algorithms to explore the extent to which the identification accuracy could be improved under different filter kernel sizes and whether combining the optimal filtering results with the original spectral bands could further enhance the accuracy. The results showed that the filter kernel size of median filtering had a significant impact on tree species identification accuracy, and that within a certain range, larger filter kernels could yield higher accuracy. In WorldView-3, the accuracy of tree species identification reached 68.95±0.68% (RF), whereas in WorldView-2, the accuracy reached 82.04±0.30% (RF) after processing with an appropriate filter kernel. When the optimal filtering features were combined with the original spectral bands, the accuracy was further improved to 68.28±0.94% in WorldView-3 (RF) and to 85±0.09% in WorldView-2 (XGBoost), representing an improvement of approximately 7% in WorldView-3 and 8% in WorldView-2 compared with the unfiltered imagery (61.64±0.35% in WorldView-3 and 77.13±0.15% in WorldView-2). The experimental results demonstrate that median filtering can effectively improve tree species classification accuracy.

Keywords: WorldView-2 and WorldView-3, median filter, tree species identification, performance evaluation, machine learning

*e-mail: gatestudy@163.com
ORCID iD: 0000-0003-0456-1545

Introduction

Forests, as a principal component of terrestrial ecosystems, represent the most biodiverse natural reservoirs and play a vital role in global carbon cycling, climate regulation, and soil and water conservation. With intensifying global climate change and increasing human activities, the sustainable management of forest resources and the conservation of biodiversity have become major issues of global concern [1]. In this context, accurately mapping the composition and distribution of forest resources – particularly achieving precise species-level distribution mapping – is of critical importance for forest inventory, ecosystem health assessment, biodiversity monitoring, and carbon sink estimation [2]. Traditional tree species surveys primarily rely on labor-intensive field investigations. While these methods yield high accuracy, they are time-consuming, costly, and difficult to implement in areas with complex terrain. Remote sensing technology, as an efficient and non-destructive Earth observation tool, provides strong technical support for large-scale tree species surveys [3]. In particular, the widespread application of high-resolution satellite imagery (such as the WorldView and GaoFen series) has made it possible to differentiate tree species with high spatial precision [4]. However, accurate species identification remains challenging due to factors such as sensor noise, atmospheric interference, shadow occlusion, and the structural complexity of forest canopies.

Currently, a substantial body of research has explored ways to improve the accuracy of tree species identification using remote sensing, primarily focusing on four main aspects. The first approach involves evaluating the performance of remote sensing data at different resolutions for species discrimination. Studies have utilized satellite imagery such as IKONOS, QuickBird, WorldView-2, and WorldView-3, as well as airborne hyperspectral data, high spatial resolution imagery, and LiDAR data [5-9]. Research indicates that high spatial resolution data, hyperspectral imagery, and the fusion of multi-source datasets significantly enhance tree species identification accuracy [10-13]. The second pathway examines the contribution of image-derived features to species classification. Spectral indices, texture features, digital surface models (DSMs), HSV color-space attributes, and three-dimensional structural features derived from LiDAR have been widely employed [14-19]. Findings suggest that all these features facilitate species discrimination, with the combined use of multiple feature types yielding the best performance [1-3, 20, 21]. The third direction investigates the influence of imaging time on identification accuracy. Studies have assessed the value of multi-temporal imagery – spanning two, three, or four seasons, as well as longer time series – in distinguishing tree species [9, 20, 22, 23]. Results demonstrate that the use of multi-season imagery considerably improves classification accuracy [3, 24, 25]. The fourth approach entails testing and developing classification methods. Research has evaluated the performance of machine learning algorithms such as maximum likelihood, support vector machines, random forest (RF), and extreme gradient boosting (XGBoost), showing that these methods achieve high accuracy in species identification [3, 6, 12, 26]. In recent years, deep learning techniques – including CNN, Transformer, LSTM, and their hybrids – have been adapted and applied to tree species recognition, significantly outperforming traditional methods and further advancing identification precision [27-30].

Although research in the aforementioned four areas has led to considerable improvements in tree species identification accuracy, remote sensing images are inevitably affected by various factors during acquisition – such as atmospheric conditions, sensor noise, and topographic shadows – which introduce varying levels of noise, particularly salt-and-pepper noise [31]. This type of noise significantly degrades image visual quality and impedes the performance of tree species classification algorithms. Therefore, effectively suppressing noise and improving image quality may represent a critical step toward further enhancing the accuracy of tree species identification. Median filtering, as a nonlinear filtering technique, offers strong noise suppression capabilities while preserving edge information. It effectively removes outliers and impulse noise from images, resulting in more robust feature representations, and has been widely used in medical imaging, industrial inspection, and remote sensing image denoising [32]. The core principle of median filtering is to replace the central pixel value with the median value of its neighborhood, which helps retain edge and detail information and avoids the edge-blurring issues commonly associated with linear filters such as mean filtering. Although median filtering is well established in general image processing, its effectiveness in improving tree species identification using high-spatial-resolution remote sensing imagery remains unclear. By reducing local noise and enhancing spectral consistency within canopy areas, median filtering has the potential to accentuate intrinsic differences in spectral responses among tree species. Consequently, integrating median filtering into tree species identification workflows may contribute to improved classification accuracy.

To explore the potential application of median filtering in tree species identification, this study utilizes WorldView-3 and WorldView-2 imagery as data sources. Multiple sets of median-filtering kernels of different sizes were constructed and applied band by band to the original images in both datasets. Using two classification methods – RF and XGBoost – we systematically evaluate the impact of different kernel sizes on species classification accuracy and determine whether median filtering can effectively improve identification performance. Given that median filtering removes outliers and generates robust features that help discriminate between tree species, whereas the original spectral bands retain high-fidelity information, we hypothesize that combining both may yield complementary benefits. This integration is expected to suppress noise while preserving critical details, potentially leading to further improvements in classification accuracy. Therefore, this study also investigates whether incorporating median-filtered features together with the original spectral bands can improve tree species identification. The findings of this research will not only contribute to a deeper understanding of the role of median filtering in tree species classification but also provide a transferable technical pathway for high-accuracy species mapping, thereby supporting intelligent monitoring and management of forest resources.

Materials and Methods

Data Sets

Remote Sensing Data

This study utilized two distinct study sites to evaluate the robustness of the proposed method. The first site, Wangcheng Park, is located in Luoyang City, Henan Province, China. This area is characterized by a warm temperate continental monsoon climate with distinct seasons and serves as a managed urban botanical garden with a diverse collection of both native and introduced tree species. The second site is situated in an urban area of Hohhot City, Inner Mongolia, China. This region experiences a semi-arid continental climate and is representative of northern China's urban afforestation patterns. The specific characteristics of remote sensing data acquired over these sites are detailed below.

The WorldView-3 imagery of the first site captured on October 27, 2017, over this botanical garden was used for the tree species identification study (Fig. 1). The image comprises a panchromatic band with a spatial resolution of 0.3 m and an 8-band multispectral image with a spatial resolution of 1.24 m. The imagery spans latitudes 34˚39′51.15″-34˚40′17.25″N and longitudes 112˚24′37.84″-112˚ 25′13.66″E, covering a total area of 0.71 km^2 [33]. Table 1 outlines the detailed parameters of this dataset.

A WorldView-2 image of the second site, captured on August 31, 2011, over this region, was used for the tree species identification study (Fig. A1 in the Appendix). The band configuration and wavelength ranges of each band in this image are identical to those of WorldView-3. However, the spatial resolution of the panchromatic band in this image is 0.5 m, whereas the spatial resolution of the 8-band multispectral image is 2.0 m. The imagery spans latitudes 40˚48′11.81″-40˚48'47.62″N and longitudes 111˚40′55.57″-111˚42′32.16″E, covering a total area of 2.45 km^2 [18, 19, 34].

Prior to use, both datasets underwent rigorous preprocessing steps, including calibration, image fusion, and atmospheric correction. In addition, the imagery used for tree species identification in this study also includes mask files created from the WorldView-3 and WorldView-2 datasets. The generation of these mask files has been detailed in previous studies [17-19, 33].

Tree Species Sample Data

For both the first and the second regions in this study, seven tree species samples were collected. Detailed

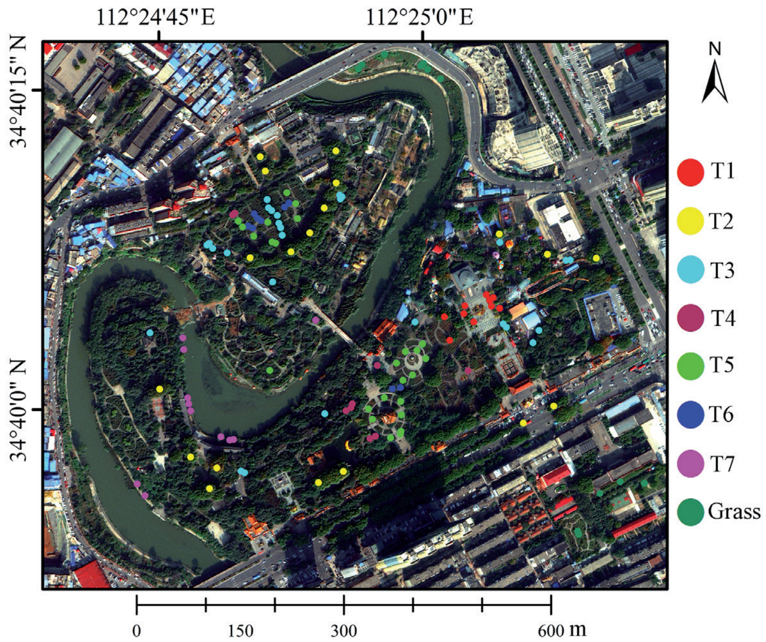

Fig. 1. WorldView-3 imagery of Wangcheng Park, where T1 to T7 represent seven tree species, and their samples, along with grass, have been labeled on the image.

Table 1. Band configuration and spatial resolution details of WorldView-3 imagery.

Band number	Band setting	Spatial resolution (m)	Wavelength range (μm)	Central wavelength
1	Coastal blue	1.24	0.40-0.45	0.425
2	Blue		0.45-0.51	0.480
3	Green		0.51-0.58	0.545
4	Yellow		0.59-0.63	0.605
5	Red		0.63-0.69	0.660
6	Red edge		0.71-0.75	0.725
7	Near-infrared 1		0.77-0.90	0.833
8	Near-infrared 2		0.86-1.04	0.950
9	Panchromatic	0.3	0.45-0.80	–

information, including the scientific names and the number of pixels for the training and validation samples, is presented in Table 2 and Table A1 (in the Appendix). The detailed procedures and methods for investigating tree species can be found in previous studies [18, 19, 33, 35].

Methodology

Median Filtering of Remote Sensing Data

Median filtering is a nonlinear digital filtering technique that effectively suppresses noise (such as salt-and-pepper noise) by replacing the central pixel value with the median of its neighboring pixels, while relatively effectively preserving image edges and fine details. The computational procedure is shown in Equation (1).

$$I_{\text{filtered}}(x, y) = \underset{(i,j)\in\Omega(x,y)}{\text{median}} \{I(i, j)\} \tag{1}$$

where I is the original input image (or spectral data); I_{filtered} is the output after median filtering; (x, y) are the coordinates of the pixel being processed; $\Omega(x, y)$ is the local window centered at (x, y); and median denotes the median operator, which sorts all pixel values within Ω and selects the middle value.

In this study, ENVI 5.4 software was used to perform median filtering on the WorldView-3 and WorldView-2 imagery. During the filtering process, the filter window size was set following a sequence of 3, 5, ..., $2N+1$, $2(N+1)+1$, where N represents the number of filtering iterations, determined when the overall classification accuracy reached an optimal level. After each filtering operation, tree species classification was performed immediately using the filtered image. By analyzing changes in overall accuracy, we determined whether further filtering with a larger window size was necessary.

Image Classification

The input data for tree species identification included the original WorldView-3 and WorldView-2 imagery, their filtered images, and the filtered images

Table 2. Scientific names of the tree species to be classified and the numbers of training and validation samples used in the classifications in Luoyang.

Tree species number	Scientific names	Training samples	Validation samples
T1	*Ginkgo biloba* L.	256	1235
T2	*Platanus orientalis*	261	1285
T3	*Platycladus orientalis* (L.)	265	1236
T4	*Cedrus deodara*	260	1248
T5	*Paeonia suffruticosa*	263	1234
T6	*Ligustrum compactum*	274	1267
T7	*Salix babylonica*	268	1271
Grass	—	271	1269

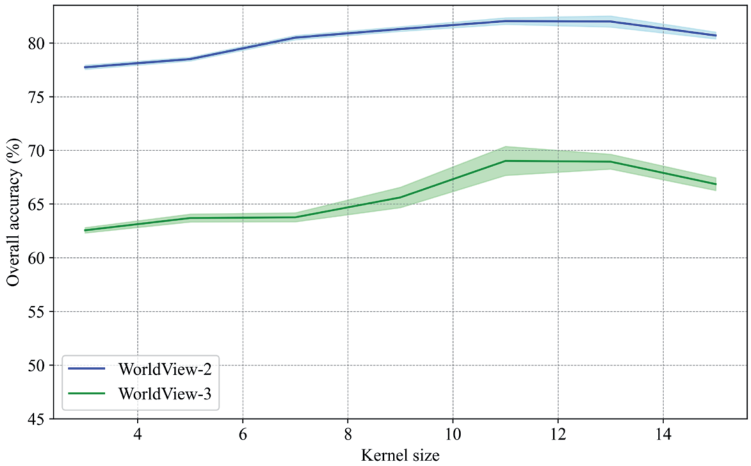

Fig. 2. Relationship between overall accuracy change and median filtering kernel size.

combined with the original spectral bands. The filtered images and the original spectral bands each consisted of eight layers, forming low-dimensional datasets. In contrast, the datasets combining filtered images and spectral bands consisted of 16 layers, forming medium-dimensional feature sets. Considering the characteristics of the datasets and the need for timely classification results, RF – known for its strong performance on both low- and high-dimensional data – and XGBoost – which also performs well across different feature dimensions – were selected to classify each image set. For each feature set, ten repeated classifications were conducted, and the mean and standard deviation of the overall accuracy were calculated to ensure the reliability of the experimental results. RF and XGBoost classifications were executed using EnMAP-Box [36] and Python-based code, respectively.

Result Evaluation

As the size of the filter window increased, the overall accuracy was used to assess its impact on tree species identification. After obtaining the optimal tree species identification results from both the median-filtered bands and the combined dataset (original bands combined with filtered bands), we compared these results with those derived from the original WorldView-3 and WorldView-2 bands to determine whether median filtering effectively improves tree species identification accuracy. A comparative analysis of the tree species identification results from the median-filtered WorldView-3 and WorldView-2 images in different regions was conducted to cross-validate the enhancement effect of median filtering on tree species identification. Based on the optimal and representative confusion matrices obtained from the classification results, the extent to which median filtering enhanced the accuracy of identifying each tree species was analyzed.

Results

Appropriate Filtering Kernel Size

The change in overall accuracy (mean ± standard deviation) of tree species classification with increasing median filter kernel size is shown in Fig. 2.

As shown in Fig. 2, the overall accuracy of tree species recognition using RF increased as the filter kernel size increased, regardless of whether WorldView-3 or WorldView-2 imagery was used. Using RF, the overall accuracy of tree species recognition reached its maximum value (68.95±0.68% for WorldView-3 and

Table 3. Overall accuracy achieved in tree species classification using eight spectral bands (SBs), median-filtered SBs (Med(SBs)), and SBs + Med(SBs) from WorldView-3 and WorldView-2 imagery.

Remote sensing sensor	WorldView-3		WorldView-2	
Classifiers	RF	XGBoost	RF	XGBoost
Data type	OA %	OA %	OA %	OA %
SBs	61.64±0.35	61.68±0.22	77.15±0.24	77.13±0.15
Med(SBs)	68.95±0.68	63.03±0.30	82.04±0.30	83.34±0.23
SBs + Med(SBs)	68.28±0.94	64.22±0.59	83.19±0.29	85.00±0.09

Table 4. Confusion matrix of tree species classification using WorldView-3 eight SBs combined with their median filtering features.

Type	T1	T2	T3	T4	T5	T6	T7	Grass	Total	User accuracy%
T1	1124	164	0	61	0	0	0	0	1349	83.32
T2	19	833	0	8	0	0	0	0	860	96.86
T3	22	0	583	215	64	0	136	0	1020	57.16
T4	0	0	565	550	37	0	56	0	1208	45.53
T5	27	0	54	50	1105	0	2	0	1238	89.26
T6	0	33	17	2	0	1026	156	405	1639	62.60
T7	15	186	17	356	28	127	893	73	1695	52.68
Grass	28	69	0	6	0	114	28	791	1036	76.35
Total	1235	1285	1236	1248	1234	1267	1271	1269	10045	
Producer accuracy%	91.01	64.82	47.17	44.07	89.55	80.98	70.26	62.33		

Note: OA = 6905/10045 = 68.74 %; KC = 0.6428.

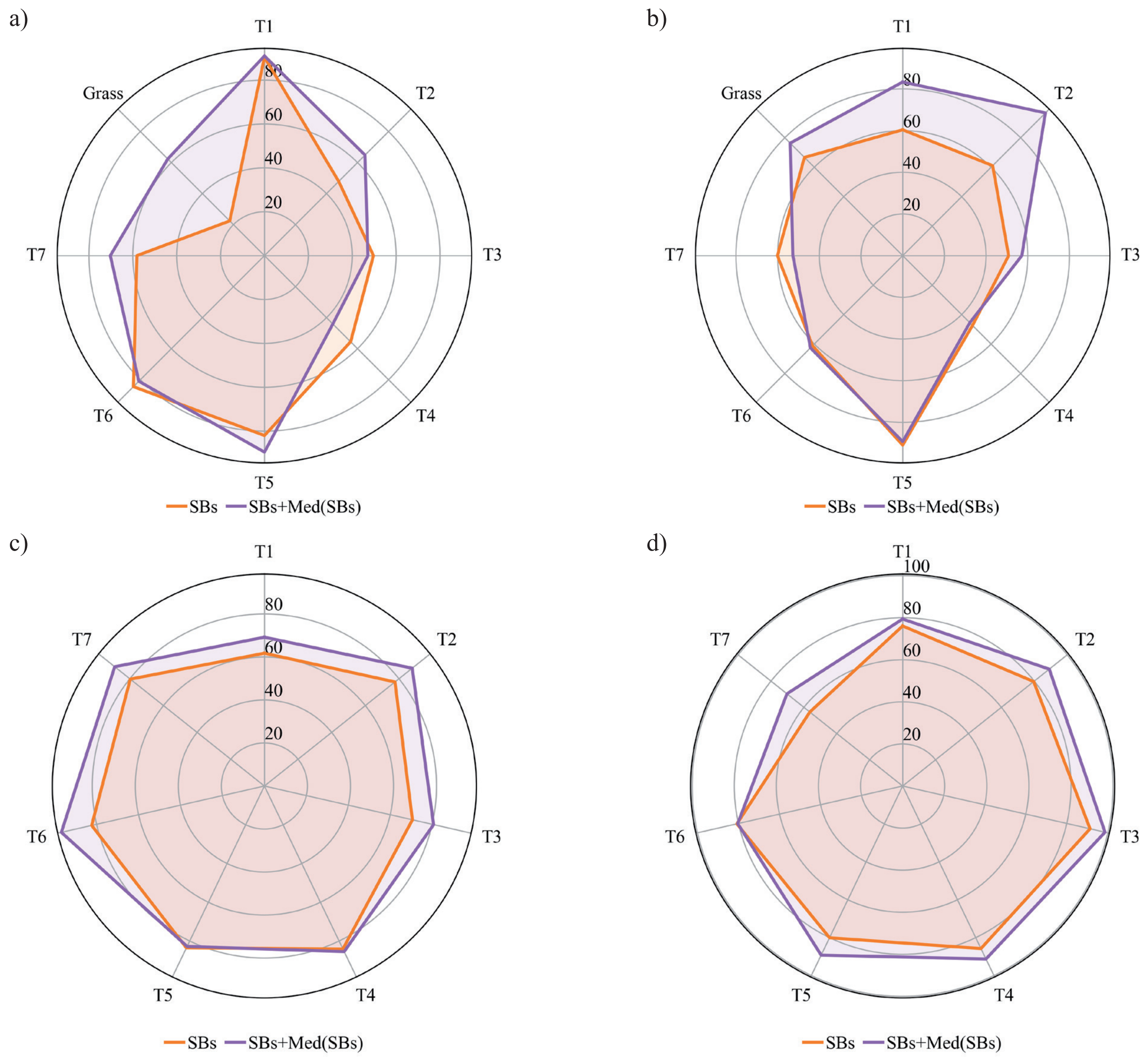

Fig. 3. Spider web graphs of producer and user accuracies in tree species identification obtained from the typical datasets. a) Producer accuracies of WorldView-3; b) user accuracies of WorldView-3; c) producer accuracies of WorldView-2; d) user accuracies of WorldView-2.

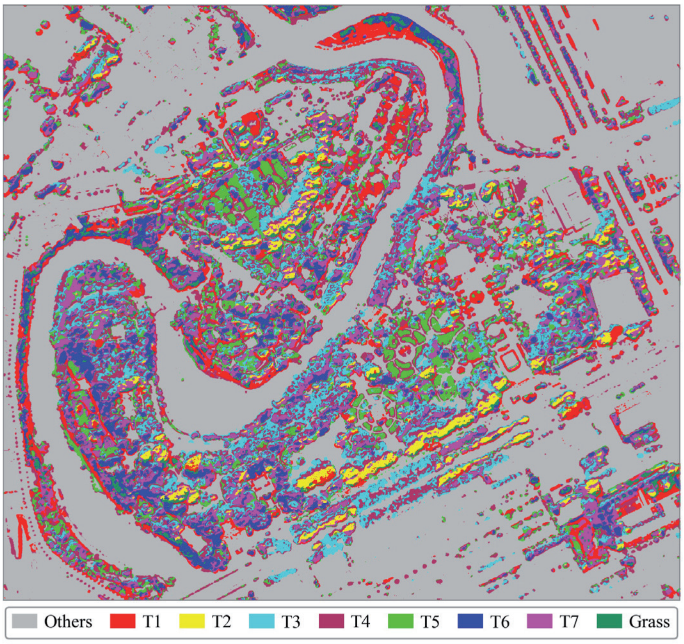

Fig. 4. Tree species classification map of WorldView-3 in Luoyang.

82.04±0.30% for WorldView-2) at relatively small kernel sizes (13 for WorldView-3 and 11 for WorldView-2).

Typical Feature Sets for Tree Species Classification

Table 3 lists the overall accuracy obtained from the typical feature sets of WorldView-3 and WorldView-2 for tree species identification, illustrating the overall improvement achieved through median filtering.

From Table 3, it can be seen that compared with the original 8-band data, the median-filtered 8-band imagery (using the optimal filtering window) significantly improves tree species recognition accuracy in both WorldView-3 and WorldView-2 datasets. The improvement in WorldView-3 is approximately 7%, while that in WorldView-2 is around 6%. Compared with the filtered feature sets alone, combining the filtered features with the original spectral bands further improves the accuracy of tree species identification. In WorldView-3, RF shows no significant improvement, whereas XGBoost shows a slight improvement; in WorldView-2, both RF and XGBoost exhibit significant improvements. The improvement in WorldView-2 was greater than that observed in WorldView-3.

Optimal Classification Result

The combination of WorldView-3 and WorldView-2 filtering features with their original spectral bands yields good results for tree species identification. The confusion matrices for one of the ten classification runs for WorldView-3 and WorldView-2 are shown in Table 4 and Table A2.

As can be seen from Table 4, except for the relatively poor identification performance of some tree species such as T3, T4, and T7, the producer and user accuracies for the remaining tree species based on the optimal median-filtered features combined with the original spectral bands in WorldView-3 both exceeded 62%. Except for tree species T2, T6, and T7, the differences between producer and user accuracies for the remaining tree species were relatively small. The overall identification performance of the seven tree species and grass was not satisfactory.

For WorldView-2 (Table A2), the producer and user accuracies of the seven tree species both exceeded 69%. The producer and user accuracies achieved for the same tree species during the identification process were not significantly different, indicating that an overall satisfactory identification performance was achieved.

Individual Tree Species Identification Effect

The spider web diagrams of producer and user accuracies obtained from tree species identification based on WorldView-3 and WorldView-2 median-filtered features combined with the original eight spectral bands, as well as the original eight spectral bands alone, are shown in Fig. 3.

From Fig. 3, it can be seen that in WorldView-3, compared with the SBs feature set, the combined feature set improved the recognition performance for T1, T2, T5, T7, and grass; however, the recognition performance for T3, T4, and T6 slightly deteriorated (producer accuracy). In terms of user accuracy, the combined feature set improved the recognition performance for T1, T2, T3, T6, and grass, while the performance for T4, T5, and T7 became slightly worse.

In WorldView-2, the identification performance for T1, T2, T3, T4, T6, and T7 using the combined feature set improved compared with the SBs feature set, while the performance for T5 became slightly worse (producer accuracy). Regarding user accuracy, the combined feature set improved the identification performance for T1, T2, T3, T4, T5, and T7, whereas the performance for T6 became slightly worse.

Using the median-filtered features combined with the original eight spectral bands of WorldView-3 and WorldView-2 for tree species classification, the best results were achieved in this study. The overall mapping results of tree species identification are shown in Fig. 4 and Fig. A2, respectively.

From Fig. 4 and Fig. A2, it can be seen that applying the median-filtered features combined with the original spectral bands resulted in more compact and homogeneous patches in tree species classification, which were more consistent with the actual distribution compared with the classification results based solely on the original spectral bands of the WorldView-3 and WorldView-2 data (which showed greater heterogeneity). The recognition performance for the various tree species was greatly improved.

Discussion

In tree species identification, the selection of the kernel size for median filtering has a crucial impact on classification accuracy. The results show that as the filtering kernel size increases, the overall accuracy of tree species recognition based on both WorldView-3 and WorldView-2 data first increases and then decreases (Fig. 2). This phenomenon indicates that an appropriate filtering kernel size can effectively remove noise and local detail interference, thereby enhancing image separability and improving classification accuracy. This shares similar characteristics with the observation that textural features extracted at an optimal window scale can effectively facilitate tree species identification [37]. The optimal filtering kernel sizes for WorldView-3 and WorldView-2 images also differ in tree species classification (Fig. 2). This difference may be related to factors such as image resolution, imaging season, and tree species distribution, all of which have been identified as critical determinants of classification performance in comparable remote sensing applications [38]. Therefore, in practical applications, an appropriate filtering kernel size should be selected based on specific data characteristics and classification requirements.

Median filtering plays an important role in improving the accuracy of tree species recognition. Its significant enhancement effect lies in its ability to effectively remove noise and outliers while preserving edge and texture information [31]. By applying median filtering, noise in the images is effectively reduced, making spectral differences between tree species more prominent and thereby improving recognition accuracy. In this study, both WorldView-3 and WorldView-2 images achieved higher tree species recognition accuracy after median filtering (Fig. 2, Table 3). This improvement is reflected not only in overall accuracy but also in the recognition performance of individual tree species (Fig. 3). Specifically, for tree species with similar spectral characteristics that are difficult to distinguish, median filtering enhances image contrast, making these species easier to identify during classification (Figs. 3, 4, and A1). Additionally, median filtering can also improve the spatial structural information of images, making homogeneous pixel clusters more continuous and complete, similar to the effect of mean texture filtering [39]. As with morphology-based filtering approaches [40], this is crucial for the utilization of spatial information in tree species recognition, contributing to improved classification accuracy. As such, median filtering serves as an effective image processing technique with significant application value in tree species recognition.

The integration of median filtering features with original spectral bands can enhance the accuracy of tree species identification (Table 3). The median filtering process effectively suppresses noise and outliers in the imagery, forming robust features for tree species recognition [32]. Meanwhile, the original spectral bands fully preserve the inherent reflectance characteristics of ground objects, which contain subtle physio-biochemical differences among tree species – such as chlorophyll content and cellular structure – that directly determine spectral signatures [31]. By combining the noise-resistant features derived from median filtering with the high-fidelity information from the original bands, this approach leverages both the improved data quality from noise suppression and the retention of critical information for species discrimination, creating a synergistic "denoising-and-fidelity-preserving" effect [41]. This multi-dimensional feature fusion strategy not only strengthens the model's resilience to complex environmental disturbances (e.g., illumination variations and atmospheric effects) but also expands the separability of the feature space through complementary feature representations. This is analogous to the well-established observation that fusing textural features with spectral features can substantially facilitate tree species identification [42]. Ultimately, this integration enables the classifier to more accurately capture spectral distinctions among different tree species, leading to a substantial improvement in recognition accuracy.

In tree species recognition, significant differences in recognition performance are observed among different tree species. These differences are not only related to the spectral characteristics and texture structures of the tree species themselves but are also influenced by multiple factors such as classifier performance, image quality, and environmental conditions [35]. Firstly, the spectral characteristics of tree species are key factors affecting recognition performance [12]. Different tree species exhibit variations in their spectral responses, which determine their distinguishability on remote sensing images. Some tree species have unique spectral features that are easily identified by classifiers, whereas others with similar spectral features are prone to misclassification (Table 3). Secondly, classifier performance also affects the recognition performance of individual tree species [3]. Different classifiers may show different advantages and disadvantages in handling different tree species. For instance, the random forest classifier excels in handling multi-class classification problems but may struggle with distinguishing certain tree species with similar spectral features (Table 3). Thirdly, factors such as image resolution and noise level affect the representation of tree species in the imagery, further influencing recognition accuracy (Fig. 2, Table 3). Additionally, environmental factors such as lighting conditions and seasonal changes can also impact the spectral characteristics of tree species, thereby affecting the recognition performance [21]. It is evident that improving the recognition accuracy of individual tree species requires comprehensive consideration of multiple factors, including spectral characteristics, classifier performance, image quality, and environmental conditions [43].

The results of this study have important implications for the application of remote sensing technology in tree species recognition. Firstly, by exploring the influence of filter kernel size on the accuracy of tree species recognition, this study provides essential information for selecting appropriate filtering parameters in practical applications. Secondly, the median filtering technique has been shown to effectively improve the accuracy of tree species recognition. This has important application value in areas such as forest monitoring and ecological assessment that rely on tree species recognition. This study provides the following two recommendations for future tree species recognition research: 1) It is necessary to select an appropriate filter kernel size based on specific data characteristics and classification requirements to optimize image quality and improve recognition accuracy; 2) It is advisable to consider using multiple classifiers to improve overall classification performance, as different classifiers may have different strengths and weaknesses in identifying various tree species.

Conclusions

This study investigated the impact of image median filtering on tree species recognition using WorldView-3 and WorldView-2 imagery. The experimental results showed that median filtering significantly enhanced the accuracy of tree species recognition. Specifically, the following observations were made: 1) As the filtering kernel size increased, the overall accuracy of tree species recognition using the RF algorithm increased, although the optimal kernel size varied depending on the image type; 2) On both WorldView-3 and WorldView-2 imagery, the accuracy of tree species recognition after median filtering with appropriate kernel sizes was higher than that obtained using the original spectral bands; 3) For tree species recognition, combining median filtering features with the original spectral bands significantly improved classification accuracy compared with using spectral bands alone, regardless of whether the RF or XGBoost algorithm was used.

While this study made meaningful discoveries, the exploration was limited to WorldView-3 and WorldView-2 imagery. In future research, other datasets such as hyperspectral imagery could be used to further explore the positive impact of median filtering combined with additional image processing techniques on tree species recognition.

Acknowledgements

This work was supported by the Scientific and Technological Project of Henan Province, China (Grant No. 262102320247), and the National Natural Science Foundation of China (Grant No. 32001250). We would like to express our gratitude to the editors and the anonymous reviewers.

AI Usage Disclosure Statement

The authors acknowledge the use of ChatGPT-4 and DeepSeek-V4 for language translation, polishing, grammar correction, and improving the written English expression in the abstract and main text to enhance readability. All AI-generated suggestions were critically reviewed, edited, and verified by the authors, who take full responsibility for the final content of the publication.

Data Availability Statement

Data are available for public use, and can be found at https://doi.org/10.5281/zenodo.20769719.

Conflicts of Interest

The authors declare no conflicts of interest.

References

1. APOSTOL B., PETRILA M., LORENT A., CICEU A., GANCZ V., BADEA O. Species discrimination and individual tree detection for predicting main dendrometric characteristics in mixed temperate forests by use of airborne laser scanning and ultra-high-resolution imagery. Science of the Total Environment, **698**, 134074, **2020**.
2. CROSS M.D., SCAMBOS T., PACIFICI F., MARSHALL W.E. Determining effective meter-scale image data and spectral vegetation indices for tropical forest tree species differentiation. IEEE Journal of Selected Topics in Applied Earth Observations and Remote Sensing, **12** (8),

2934, **2019**.
3. LIU H. Classification of tree species using UAV-based multi-spectral and multi-seasonal images: a multi-feature-based approach. New Forests, **55** (1), 173, **2024**.
4. PU R., LANDRY S. A comparative analysis of high resolution IKONOS and WorldView-2 imagery for mapping urban tree species. Remote Sensing of Environment, **124**, 516, **2012**.
5. NAIDOO L., CHO M.A., MATHIEU R., ASNER G.P. Classification of savanna tree species, in the Greater Kruger National Park region, by integrating hyperspectral and LiDAR data in a Random Forest data mining environment. ISPRS Journal of Photogrammetry and Remote Sensing, **69** (3), 167, **2012**.
6. GHOSH A., JOSHI P.K. A comparison of selected classification algorithms for mapping bamboo patches in lower Gangetic plains using very high resolution WorldView-2 imagery. International Journal of Applied Earth Observation and Geoinformation, **26** (1), 298, **2014**.
7. FERREIRA M.P., WAGNER F.H., ARAGAO L.E.O.C., SHIMABUKURO Y.E., FILHO C.R.D.S. Tree species classification in tropical forests using visible to shortwave infrared WorldView-3 images and texture analysis. ISPRS Journal of Photogrammetry and Remote Sensing, **149**, 119, **2019**.
8. HAMRAZ H., JACOBS N.B., CONTRERAS M.A, CLARK C. Deep learning for conifer/deciduous classification of airborne LiDAR 3D point clouds representing individual trees. ISPRS Journal of Photogrammetry and Remote Sensing, **158**, 219, **2019**.
9. SHI Y.F., WANG T.J., SKIDMORE A.K., HEURICH M. Improving LiDAR-based tree species mapping in Central European mixed forests using multi-temporal digital aerial colour-infrared photographs. International Journal of Applied Earth Observation and Geoinformation, **84**, 101970, **2020**.
10. ZHANG Z., KAZAKOVA A., MOSKAL L.M., STYERS D.M. Object-based tree species classification in urban ecosystems using LiDAR and hyperspectral data. Forests, **7** (6), 122, **2016**.
11. TORABZADEH H., LEITERER R., HUENI A., SCHAEPMAN M., MORSDORF F. Tree species classification in a temperate mixed forest using a combination of imaging spectroscopy and airborne laser scanning. Agricultural and Forest Meteorology, **279**, 107744, **2019**.
12. MODZELEWSKA A., FASSNACHT F.E., STERENCZAK K. Tree species identification within an extensive forest area with diverse management regimes using airborne hyperspectral data. International Journal of Applied Earth Observation and Geoinformation, **84**, 101960, **2020**.
13. KUREEL N., SARUP J., MATIN S., GOSWAMI S., KUREEL K. Modelling vegetation health and stress using hyperspectral remote sensing data. Modeling Earth Systems and Environment, **8**, 733, **2022**.
14. WANG T., ZHANG H., LIN H., FANG C. Textural-spectral feature-based species classification of mangroves in mai po nature reserve from Worldview-3 imagery. Remote Sensing, **8** (1), 24, **2016**.
15. ÅKERBLOM M., RAUMONEN P., MAKIPAA R., KAASALAINEN M. Automatic tree species recognition with quantitative structure models. Remote Sensing of Environment, **191**, 1, **2017**.
16. YU X., HYYPPA J., LITKEY P., KAARTINEN H., VASTARANTA M., HOLOPAINEN M. Single-sensor solution to tree species classification using multispectral airborne laser scanning. Remote Sensing, **9** (2), 108, **2017**.
17. LIU H., AN H. Urban greening tree species classification based on HSV colour space of WorldView-2. Journal of the Indian Society of Remote Sensing, **47** (11), 1959, **2019**.
18. LIU H., AN H. Analysis of the importance of five new spectral indices from WorldView-2 in tree species classification. Journal of Spatial Science, **65** (3), 455, **2020**.
19. LIU H. Effectiveness of the spectral area index created by three algorithms for tree species recognition. Annals of Forest Science, **80**, 17, **2023**.
20. LIU H. Classification of urban tree species using multi-features derived from four-season RedEdge-MX data. Computers and Electronics in Agriculture, **194**, 106794, **2022**.
21. LIU H. Spectral volume index creation and performance evaluation: a preliminary test for tree species identification. Heliyon, **9** (6), e17203, **2023**.
22. PU R., SHAWN L., YU Q. Assessing the potential of multi-seasonal high resolution pléiades satellite imagery for mapping urban tree species. International Journal of Applied Earth Observation and Geoinformation, **71**, 144, **2018**.
23. MASEMOLA C., CHO M.A., RAMOELO A. Assessing the effect of seasonality on leaf and canopy spectra for the discrimination of an alien tree species, acacia mearnsii, from co-occurring native species using parametric and nonparametric classifiers. IEEE Transactions on Geoscience and Remote Sensing, **57** (8), 5853, **2019**.
24. HAN W., ZHANG S., JIAO Q., WU H. Dominant tree species mapping based on multi-temporal CHRIS hyperspectral satellite data. Forest Inventory and Planning, **44** (2), 1, **2019** [In Chinese].
25. IMMITZER M., NEUWIRTH M., BOCK S., BRENNER H., VUOLO F., ATZBERGER C. Optimal input features for tree species classification in central europe based on multi-temporal sentinel-2 data. Remote Sensing, **11** (22), 2599, **2019**.
26. RICHARDS J.A., JIA X. Using suitable neighbors to augment the training set in hyperspectral maximum likelihood classification. IEEE Geoscience and Remote Sensing Letters, **5** (4), 774, **2008**.
27. KEMAL A., SERHAT K., ONUR C. Classification and diagnosis of cervical cancer with stacked autoencoder and softmax classification. Expert Systems with Applications, **115**, 557, **2019**.
28. ZHANG B., ZHAO L., ZHANG X. Three-dimensional convolutional neural network model for tree species classification using airborne hyperspectral images. Remote Sensing of Environment, **247**, 111938, **2020**.
29. CARVALHO M.D., MARCATO J., MARTINS J.A.C., ZAMBONI P., COSTA C.S., SIQUEIRA H.L., ARAUJO M.S., GONCALVES D.N., FURUYA D.E.G., OSCO L.P., RAMOS A.P.M., LI J., CASTRO A.A.D., GONCALVES W.N. A deep learning-based mobile application for tree species mapping in RGB images. International Journal of Applied Earth Observation and Geoinformation, **114**, 103045, **2022**.
30. KWON R., RYU Y., YANG T., ZHONG Z.L., IM J. Merging multiple sensing platforms and deep learning empowers individual tree mapping and species detection at the city scale. ISPRS Journal of Photogrammetry and Remote Sensing, **206**, 201, **2023**.
31. PU R. Mapping tree species using advanced remote sensing technologies: a state-of-the-art review and perspective. Journal of Remote Sensing, **2021**, 9812624,

2021.
32. AHMED S., ISLAM S. Methods in detection of median filtering in digital images: a survey. Multimedia Tools and Applications, **82**, 43945, **2023**.
33. LIU H., WU J., LI X., LIU Y., SATYBALDIEVNA C.D. Tree species identification using principal component analysis features: an analysis on whether non-vegetation components should be excluded. Applied Ecology and Environmental Research, **23** (1), 1675, **2025**.
34. LIU H., AN H. Extraction of four types of urban ground objects based on a newly created WorldView-2 multi-colour spectral index. Journal of the Indian Society of Remote Sensing, **48** (7), 1091, **2020**.
35. LIU H.P., AN H.J., WANG B., ZHANG Q.L. Tree species classification using WorldView-2 images based on recursive texture feature elimination. Journal of Beijing Forestry University, **37** (8), 53, **2015** [In Chinese].
36. VAN DER LINDEN S., RABE A., HELD M., JAKIMOW B., LEITAO P.J., OKUJENI A., SCHWIEDER M., SUESS S., HOSTERT P. The EnMAP-box- A toolbox and application programming interface for EnMAP data processing. Remote Sensing, **7** (9), 11249, **2015**.
37. WU Y., ZHANG X. Object-oriented tree species classification with multi-scale texture features based on airborne hyperspectral images. Journal of Beijing Forestry University, **42** (6), 91, **2020** [In Chinese].
38. SUN M., ZHOU C.G., ZOU C.X., ZHANG Z.N., LIU D. Land type information extraction and landscape pattern dynamic analysis of Laoshan scenic area. Journal of Ecology and Rural Environment, **36** (2), 211, **2020** [In Chinese].
39. WANG X.F., WANG Y., ZHOU C.W., YIN L.C., FENG X.M. Urban forest monitoring based on multiple features at the single tree scale by UAV. Urban Forestry & Urban Greening, **58**, 126958, **2021**.
40. TIAN X.M., CHEN L., ZHANG X.L. Classifying tree species in the plantations of southern China based on wavelet analysis and mathematical morphology. Computers and Geosciences, **151**, 104757, **2021** [In Chinese].
41. ZHOU X.S., YANG W.N., LUO K., PIAO H.Y., ZHOU T., ZHOU J., TANG X.L. Research on UAV hyperspectral of tree species classification based on machine learning algorithms and spatial resolution adjustment. Remote Sensing Technology and Application, **39** (4), 880, **2024**
42. HE G., WU T.J. Hyperspectral image classification employing spatial-spectral feature supported by 3D convolution and transformer. Computer Engineering and Applications, **61** (2), 259, **2025** [In Chinese].
43. LIU H.P. Optimal coupling model for tree species identification using derivative calculation and texture filtering. Urban Forestry & Urban Greening, **117**, 129296, **2026**.

Appendix

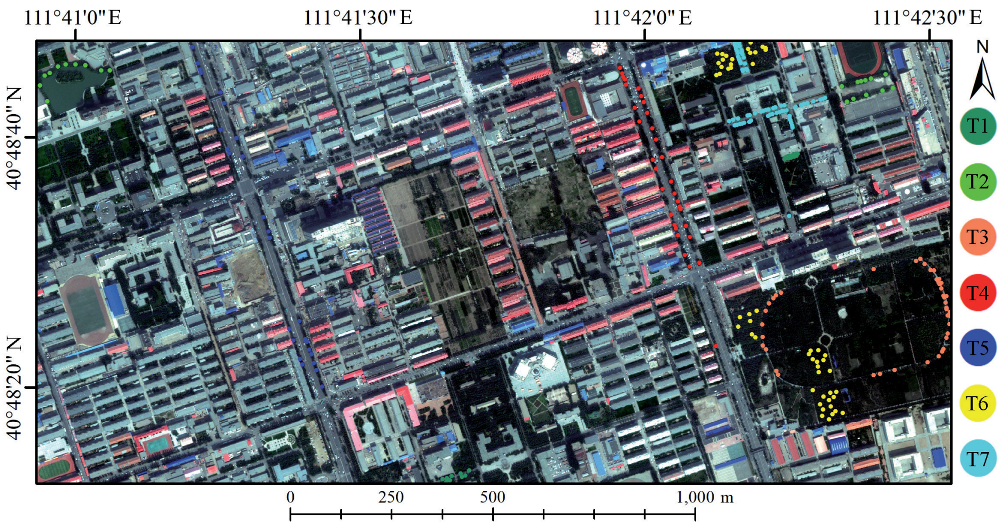

Fig. A1. WorldView-2 image of the study area (true color, with the RGB channels loaded with the bands 5, 3, and 2, respectively). The spatial distribution of seven tree species (T1-T7 represent the seven tree species) is indicated by different colors in the imagery.

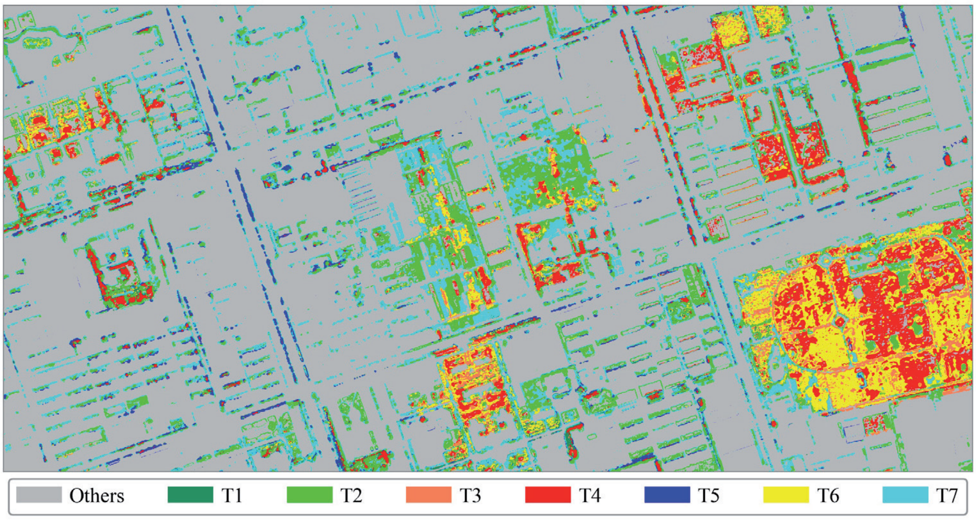

Fig. A2. Tree species classification map derived from WorldView-2 imagery in Hohhot.

Table A1. Scientific names and the number of pixels for the training and validation samples of the classified tree species in Hohhot.

Tree species number	Scientific name	Training samples	Validation samples
T1	*Salix babylonica*	1107	1229
T2	*Sophora japonica*	1047	1246
T3	*Populus alba* var. *Pyramidalis*	1066	1250
T4	*Pinus tabulaeformis*	1064	1218
T5	*Picea meyeri*	614	968
T6	*Sabina chinensis*	1019	1016
T7	*Juniperus rigida*	1047	1149

Table A2. Confusion matrix of tree species classification using the eight WorldView-2 SBs combined with their median filtering features.

Type	T1	T2	T3	T4	T5	T6	T7	Total	User accuracy%
T1	670	9	29	30	18	2	86	844	79.38
T2	1	1080	0	120	0	8	3	1212	89.11
T3	1	0	927	0	0	5	7	940	98.62
T4	1	74	0	1065	24	3	0	1167	91.26
T5	100	0	0	9	1035	7	9	1160	89.22
T6	24	18	169	21	49	1179	7	1467	80.37
T7	171	48	24	1	124	14	904	1286	70.30
Total	968	1229	1149	1246	1250	1218	1016	8076	
Producer accuracy%	69.21	87.88	80.68	85.47	82.80	96.80	88.98		

Note: OA = 6819/8076 = 84.94%; KC = 0.8241.